

Electronic Supplementary Information (ESI)

Optimization of analytical assay performance of antibody-gated indicator releasing mesoporous silica particles

Elena Costa, Estela Climent, Kornelia Gawlitza, Wei Wan, Michael G. Weller, Knut Rurack*

Bundesanstalt für Materialforschung und –prüfung (BAM), Richard-Willstätter-Str. 11, D-12489 Berlin, Germany

Table of contents

S1. Reagents and general techniques	S2
S2. Syntheses	S3
S3. Materials characterisation.....	S7
S4. Relative measurement uncertainties and limits of detection (LOD).....	S12
S5. NMR and MS spectra	S18
S6. References	S24

S1. Reagents and general techniques

Chemicals and solvents were purchased from Sigma-Aldrich, ACBR, Merck and J.T. Baker in the highest quality available. The monoclonal anti-pyrethroids antibody (clone number PY-1) was purchased from Abraxis (now Eurofins). Buffers were prepared with ultrapure reagent water, which was obtained by running demineralized water (by ion exchange) through a Milli-Q® ultrapure water purification system (Millipore Synthesis A10). Phosphate-buffered saline of 10, 50 and 80 mM (e.g., PBS 80 mM: 70 mmol L⁻³ Na₂HPO₄, 10 mmol L⁻³ NaH₂PO₄, 145 mmol L⁻³ NaCl, pH 7.5) were used for the capping processes. Controlled release experiments were performed using a solution of PBS (80 mM) containing 10% of *i*-propanol (iPrOH). Glass fibre membranes (GF/C grade) were purchased from Whatman and the sample pad membrane employed (Ahlstrom Grade 142 microfiber glass) was provided by Kenosha.

UV/vis and fluorescence spectroscopy, elemental analysis, transmission and scanning transmission electron microscopy (TEM and STEM), N₂ adsorption-desorption, mass spectrometry, and nuclear magnetic resonance (NMR) techniques were employed to characterize the synthesized compounds and materials and to test their behaviour towards the model analytes. UV/vis spectra were measured with a Specord 210 plus from Analytik Jena. Fluorescence measurements were carried out on a Fluoromax4 from HORIBA Scientific. Elemental analyses were performed on a Euro EA-Elementaranalysator. Thermogravimetric analyses were carried out on a STA7200 (Hitachi High-Tech Analytical Science) thermobalance, using in a first step a nitrogen atmosphere (80 mL min⁻¹) with a heating program consisting of a ramp of 10 °C min⁻¹ from 25 °C to 600 °C and in a second step an oxidizing atmosphere (air, 80 mL min⁻¹) from 600 °C until 1000 °C with a heating program consisting of a ramp of 10 °C min⁻¹. TEM images and STEM scans, as well as energy-dispersive X-ray spectroscopy (EDX) analyses, were performed with a Talos F200S scanning/transmission electron microscope, ThermoFisher Scientific. N₂ adsorption/desorption isotherms were recorded with a Micromeritics ASAP2010 automated sorption analyser. The solid materials prepared were calcinated in a Muffle furnace of Nabertherm. Mass spectra were measured with an Orbitrap Exactive ESI-HRMS. ¹H and ¹³C nuclear magnetic resonance (NMR) spectra were acquired with Bruker AV-500 and AV-600 spectrometers using residual protonated solvents as internal standards (¹H: δ[CDCl₃] = 7.24 ppm and ¹³C: δ[CDCl₃] = 77.23 ppm). A lateral flow dispenser from ClaremontBio® was used to dispense the APTES-functionalised MCM-41 nanoparticles in the focussing area in the detection zone of the strips.¹ A 3D-box was printed with black PLA using an Ultimaker 3 printer.¹ LEDs and optical filters were purchased from Thorlabs. Photographs were taken with a Samsung Galaxy S7 and values of the integrated density were obtained with the software ImageJ. The smartphone camera was set to a shutter speed of 1/100 s, a white balance at 4000 K, a Macro Focus and an ISO value of 100.

S2. Syntheses

Synthesis of 3-phenoxybenzoic acid silane derivative I.² In a first step, 0.5 mL of anhydrous THF solutions of *N*-hydroxysuccinimide (NHS, 138.1 mg; 1.2 mmol) and *N,N'*-dicyclohexylcarbodiimide (DCC, 247.2 mg; 1.2 mmol) were prepared. Then, each solution was added to a solution of 3-PBA (214.3 mg, 1 mmol) in anhydrous THF (1.25 mL). The mixture was stirred at room temperature for 2 h, and the white solid formed (dicyclohexylurea) was removed by centrifugation and was washed with 0.75 mL THF, with the aim to recover the residual active ester on the precipitate. The mixture was stirred for another 4 h at room temperature, centrifuged and washed with 1 mL THF. The solution was divided into 3 fractions of 1.2 mL, each of them containing ca. 0.3 mmol of active ester. In a second step, (3-aminopropyl)triethoxysilane (70.2 μ L, 250 μ mol) was added to one of the fractions, and the reaction mixture was stirred for 20 h at room temperature. The solution was centrifuged, and after the product formed, it was left in 1 mL THF. The formation of the hapten derivative was confirmed by UPLC-HRMS and NMR. Exact mass $C_{20}H_{32}NO_3Si$ $[M+H]^+$ 418.2050; found 418.2162. 1H NMR ($CDCl_3$, 400 MHz) δ 0.70 (t, 2H, $-CH_2Si$), 1.205 (t, 9H, $-OCH_2CH_3$), 1.74 (tt, 2H, CH_2CH_2Si), 3.44 (t, 2H, $-NHCH_2CH_2Si$), 3.80 (q, 6H, $-OCH_2CH_3$), 7-7.9 (9H). ^{13}C NMR ($CDCl_3$, 400 MHz) δ 7.8 (1C, $-CH_2Si$), 18.3 (3C, $-OCH_2CH_3$), 25.4 (1C, $-NHCH_2CH_2Si$), 43 (1C, $-NHCH_2CH_2Si$), 58.4 (3C, $-OCH_2CH_3$), 117 (1C, *Car*), 119 (3C, *Car*), 121 (1C, *Car*), 123 (1C, *Car*), 129 (3C, *Car*), 136 (1C, *Car*), 156 (1C, *Car*), 157 (1C, *Car*), 167 (1C, $NHCO$).

Synthesis of 3-phenoxybenzoic acid silane derivative II. 3-PBA silane derivative II was synthesized as recently described by us in ref. ¹. In brief, solutions of *N*-hydroxysuccinimide (NHS, 138.1 mg; 1.2 mmol) and *N,N'*-dicyclohexylcarbodiimide (DCC, 247.2 mg; 1.2 mmol) in 0.5 mL anhydrous THF were added to a 3-PBA (214.3 mg, 1 mmol) solution in 1.25 mL anhydrous THF, stirred at room temperature for 2 h, and dicyclohexylurea formed as a white solid was removed by centrifugation. After washing with 0.75 mL THF and stirring for another 4 h at room temperature, the suspension was centrifuged and washed with 1 mL THF. Subsequently, 3-(ethoxydimethylsilyl) propylamine (210 μ L, 0.9 μ mol) was added, and the reaction mixture stirred for 20 h at room temperature. After centrifugation, the product was re-suspended in 1.5 mL THF. Exact mass $C_{20}H_{28}NO_3Si$ $[M+H]^+$ 358.1838; found 358.1866. 1H -NMR ($CDCl_3$, 400 MHz) δ 0.11 (s 6H $-(CH_3)_2$ Si), 0.65 (t, 2H, $-CH_2Si$), 1.17 (t, 3H, $-OCH_2CH_3$), 1.65 (tt, 2H, $-CH_2CH_2Si$), 2.82 (q, 2H, $-OCH_2CH_3$), 3.43 (t, 2H, $-NHCH_2CH_2Si$), 7-7.9 (9H).

Synthesis of MCM-41 mesoporous silica nanoparticles (S1).³ *N*-Cetyltrimethylammonium bromide (CTAB, 1.00 g, 2.74 mmol) was first dissolved (slowly stirred at 30–35 °C) in deionized water (480 mL). Then, 3.5 mL NaOH (2 M) were added to the CTAB solution, followed by adjusting the temperature to 80 °C. The solution was vigorously stirred, and tetraethylorthosilicate (TEOS, 5.00 mL; 25.7 mmol) was added dropwise to the surfactant solution. During the addition of TEOS, the formation of a white precipitate was observed. The mixture was stirred for 2 h. Finally, the solid product was centrifuged (20 min at 8500 rpm), washed with deionized water and ethanol (mixture ca. 2:1 H₂O: EtOH each time) until neutral pH, and dried at 60 °C overnight. To prepare the final porous material **S1**, the as-synthesized solid was calcinated by ramping for 2 °C min⁻¹ until 550 °C and leaving the solid at 550 °C for 5 h, using an oxidizing atmosphere to remove the template phase.

Synthesis of long SBA-15 fibres (S2). Rod-shaped SBA-15 was synthesized as recently described by us in ref. ¹, using a triblock poly (ethylene oxide)–poly (propylene oxide)–poly (ethylene oxide) (P123, Aldrich, M_n = 5800 g mol⁻¹) copolymer as a structure-directing agent and TEOS as a silica source. 4.0 g (0.69 mmol) P123 were dissolved in a mixture of 120 mL water and 19.41 mL HCl conc. under stirring at 50 °C for 1 h. Afterwards, 9.15 mL TEOS (41 mmol) were added dropwise into the solution while stirring was continued at 35 °C for 24 h. The resulting gel was aged at 115 °C in a polypropylene flask under static conditions for another 24 h. The white solid obtained (**S2**) was centrifuged, washed five times with distilled water and air-dried at 115 °C in a vacuum for 48 h.

Synthesis of SBA-15 platelets (S3).⁴ 1.0 g (0.17 mmol) P123 was dissolved in 40 mL HCl (2 M) and then stirred at 35 °C for 30 min to dissolve the polymer. Afterwards, first 165 mg ZrOCl₂·8H₂O (0.5 mmol) and then 2.25 mL TEOS (10 mmol) were added dropwise into the homogeneous solution while stirring at 35 °C for 24 h. The obtained gel was aged at 100 °C in a polypropylene flask under static conditions for another 24 h. The white solid obtained (**S3**) was centrifuged, washed 5-times with distilled water and air-dried at 70 °C in a vacuum for 48 h.

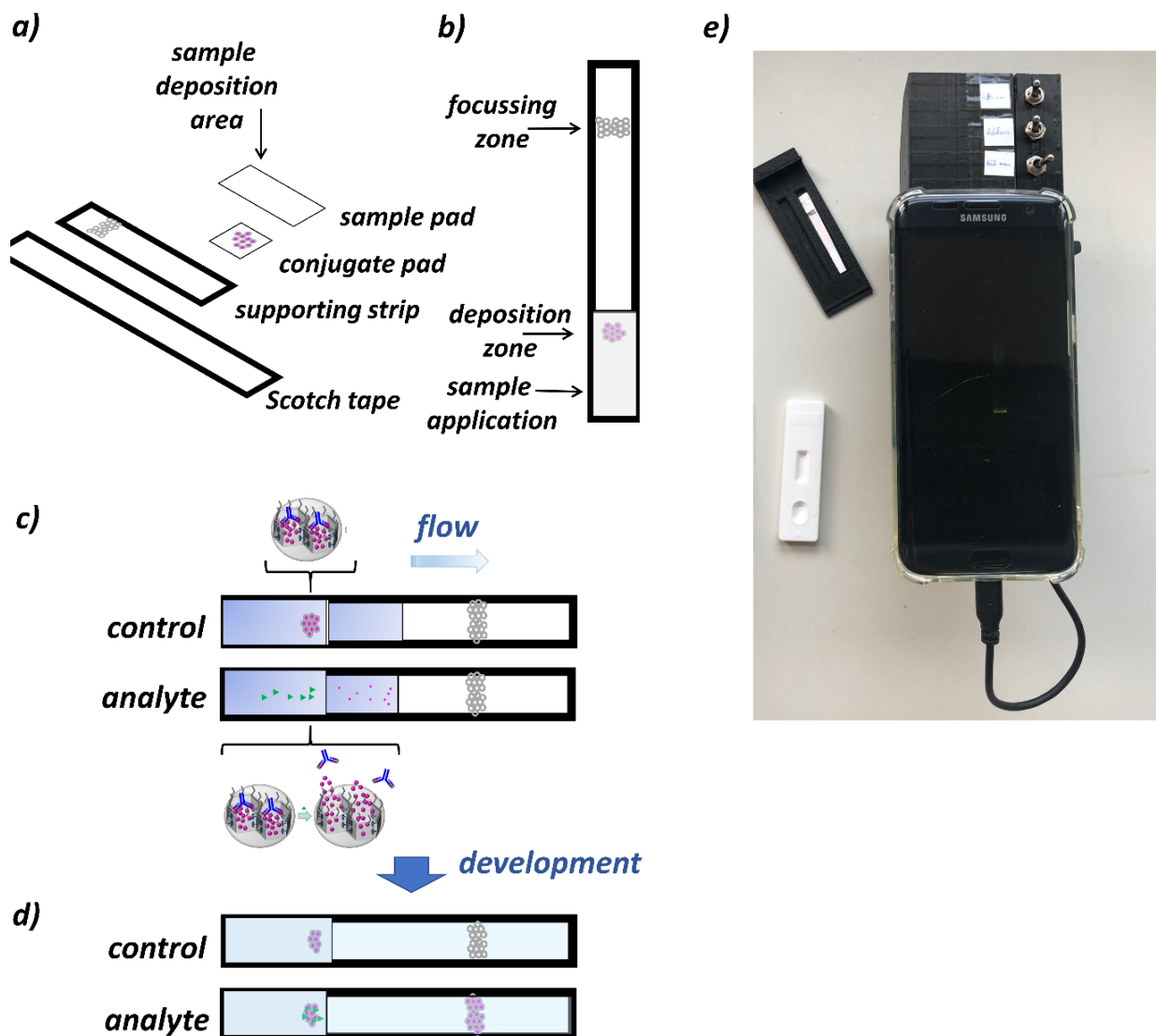
Synthesis of long SBA-15 fibres with larger pores (S4).⁵ In a typical synthesis, two solutions were prepared, the first one containing 2.0 g (0.35 mmol) P123 in 75 mL HCl (1.6 M) and the second one containing 1.0 g (0.17 mmol) P123 in 75 mL HCl (1.6 M). The solutions were stirred 1 h at 40 °C. Afterwards, 4.3 g TEOS were added to the first solution, left stirring at 40 °C during 65 min (a precipitate starts to appear after 30 min) whereas the second solution was also left at 40 °C yet nothing was added. After 65 min, the solid present in solution 1 was centrifuged and added to the second solution. Stirring was continued before adding 2 g 1,3,5-trimethylbenzene (TMB). The

suspension was left to stir for 24 h at 40 °C. The resulting gel was aged at 115 °C in a polypropylene flask under static conditions for another 48 h. The white solid obtained (**S4**) was centrifuged, washed 5-times with distilled water and air-dried at 70 °C in a vacuum for 48 h.

Synthesis of SBA-16 microparticles (S5).⁶ Silica-block copolymer SBA 16-type material was synthesized using poly(ethylene-oxide)-block-poly(propylene-oxide)-block-poly(ethylene-oxide) (Pluronic F127, $M_{av} = 12600 \text{ g mol}^{-1}$) as a structure-directing agent. 3.0 g Pluronic P127 was dissolved in 144 mL water and 13.9 mL HCl (38%) solution under vigorous stirring at 25 °C. After approx. 30 min, 11 mL of the co-surfactant butanol (BuOH) was added to achieve a 1:3 (F127:BuOH) mass ratio in the ternary system. Next, 15.3 mL TEOS were added to the solution while stirring at 45 °C for 24 h. The obtained gel was aged at 100 °C in a polypropylene flask under static conditions for another 24 h. Afterwards, the solid (**S5**) was washed with distilled water, collected by filtration and dried at 40° C.

PEG-coating of glass fibre strips. PEG-coating of the glass fibre strips was carried out as recently described by us in ref. ¹ by adding 0.57 mL water (Milli-Q®), 1.23 mL EtOH abs., 300 µL TEOS, 200 µL PEGs and 30 µL NH₃ (32 % soln.) in this order to ca. 10 glass fibre strips of 5 × 0.5 cm, located in a vial, and left under rotation overnight. Subsequently, the strips were washed three times with EtOH abs. and dried in a vacuum oven for 3 h.

Strip assembly. The strips used for the dip stick model assays were assembled as recently described by us in ref. ¹. Scheme S1 illustrates the approach. The AGIR materials **S1.2**, **S2a-AB**, **S3a-AB**, **S4a-AB** or **S5a-AB** were deposited by pipetting of a suspension (2.5 µL of a solution of 1 mg **S1-AB** in 1 mL PBS) onto the conjugate pad previously modified with PEG silanes, see above, before sandwiching this pad between the basal glass fibre carrier membrane and a glass fibre sample pad. An APTES-modified MCM-41-type material **APTES-MCM** was applied to the strip as a line in the detection zone with a lateral flow dispenser, for focussing the released indicator.



Scheme S1. The architecture of strip and principle of the lateral flow assay. (a) Assembly of layers at the sample application and interaction side of the strip; (b) top view of the different zones of the strip, i.e., deposition zone of capped material, zone to focus the released dye through APTES-modified MCM-41 nanoparticles for better detection and sample application area; (c) scenario in mid-flow, after pipetting a sample on the sample pad. No release occurs in the absence of analyte, yet dye is released in its presence, travels to focusing zone where it is trapped through electrostatic interactions (d). (e) Photograph of the macroscopic assay components with strip, lateral flow cassette, 3D-printed case with excitation sources and optics, and smartphone.

S3. Materials characterisation

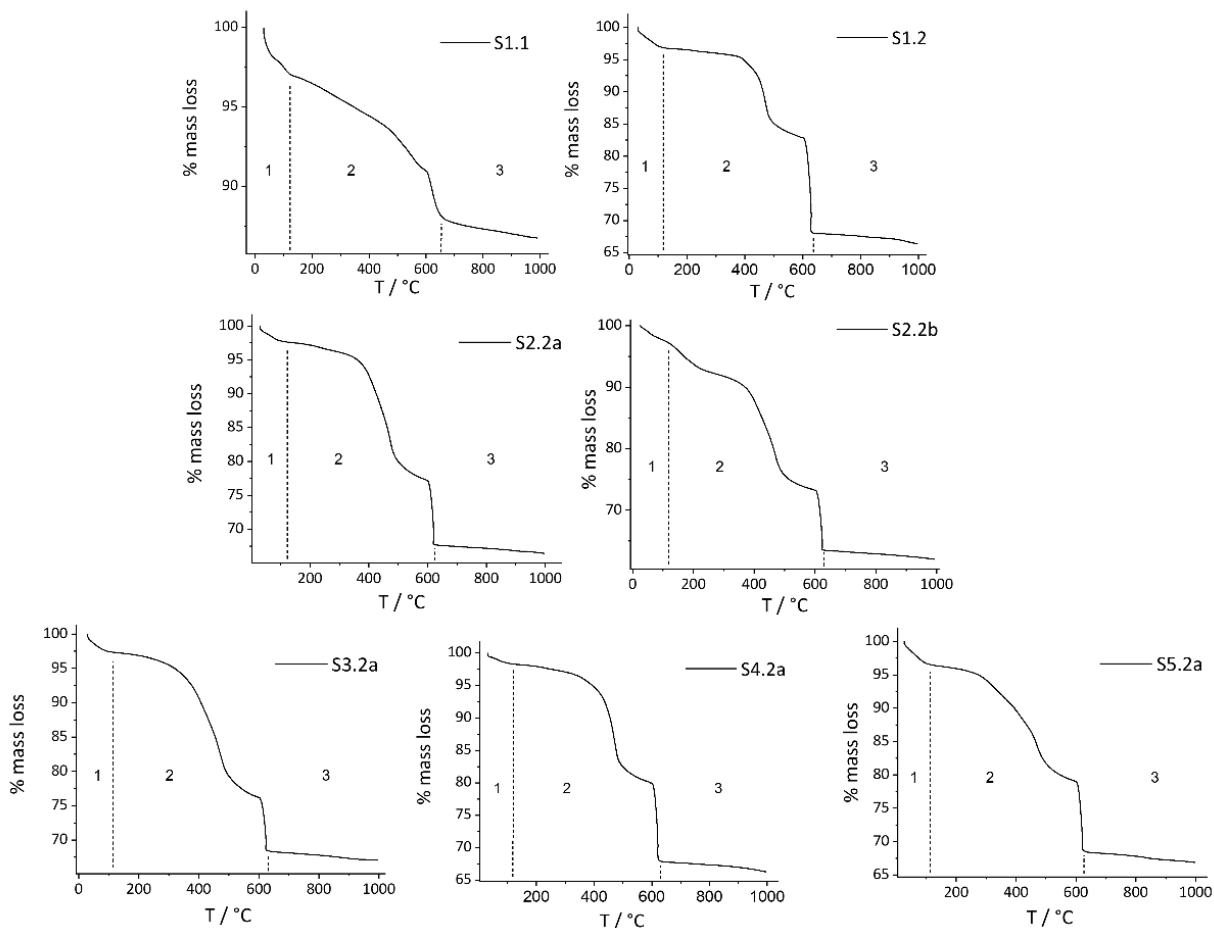


Fig. S1. TGA plots of the materials prepared. Zone 1: loss of residual water (until ca. 120 °C); zone 2: loss of organic matter (ca. 120–630 °C); zone 3: silanol condensation (above ca. 630 °C). With the ramping program used, at 600 °C the nitrogen flow is substituted by an oxygen flow, forcing the combustion of the residual organic matter and entailing a sudden step in the graphs.

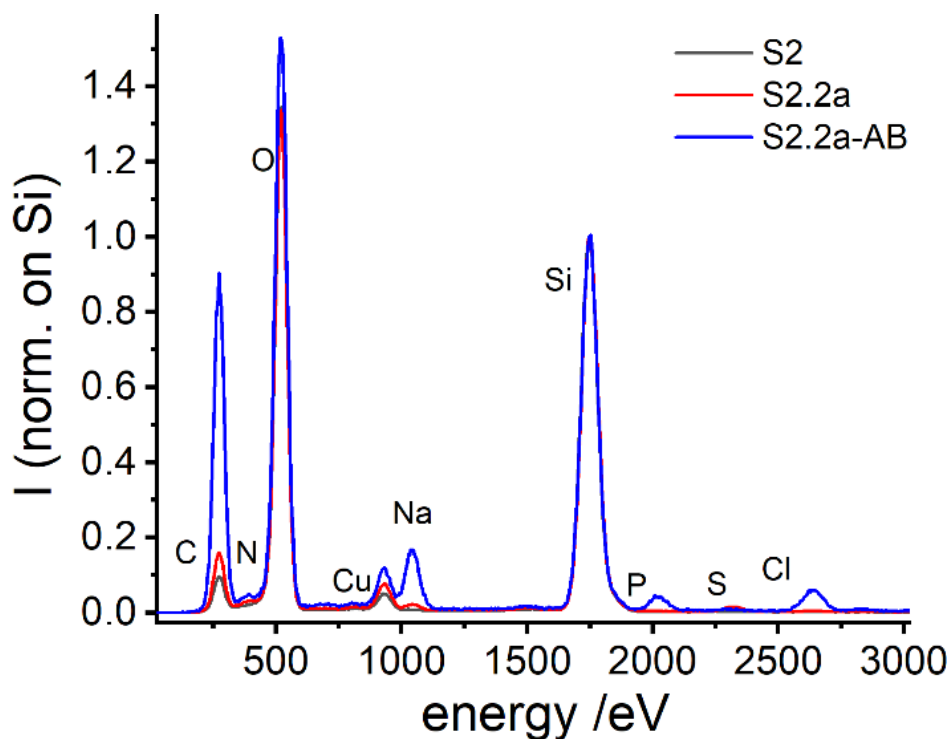


Fig. S2 Energy-dispersive X-ray (EDX) spectra of materials **S2**, **S2.2a**, and **S2.2a-AB** from TEM.

Dye loss during capping. When considering the overall shape and size of an antibody as a cap, it is obvious why even for the best performing material, ca. 40% of the initially loaded indicator is lost during the washing steps after capping and that this value increases up to >90% for ill-fitting caps. The walls of surfactant-templated mesoporous silica materials are too thin to allow for tight closing of all pores, even if a cap perfectly matches a pore opening. Antibodies, with their typical Y-shaped structure, even when perfectly binding with one binding site into a single pore opening, are too bulky, preventing an efficient closing of the next-neighbouring pores. The dyes residing in these pores, as well as any dye that is adsorbed to the non-porous parts of a particle's surface, have to be washed away after capping because otherwise, blank release in the absence of analyte would always be an issue. Here, the relative dye losses during washing were determined to $42 \pm 3\%$ for **S2.2a-AB**, **S2.2b-AB** and **S5.2a-AB**, 57% for **S4.2a-AB** and 65% for **S3.2a-AB**. For the MCM-based, narrower-pore material loaded with SRG, **S1.2-AB**, this value still amounts to 28%.

Table S1. Amounts of the average (χ) and standard deviation (σ) of C, Na, P, and S (in mmol g⁻¹ SiO₂) estimated through EDX analysis for the materials S2, S2.2a, and S2.2a-AB.

	C	Na	P	S
S2; χ	11.44	0.01	0.03	0.00
S2; σ	5.80	0.03	0.02	0.00
S2.2a; χ	14.74	0.18	0.03	0.14
S2.2a; σ	8.93	0.10	0.02	0.15
S2.2a-AB; χ	34.72	2.85	0.68	0.03
S2.2a-AB; σ	9.75	1.41	0.23	0.03

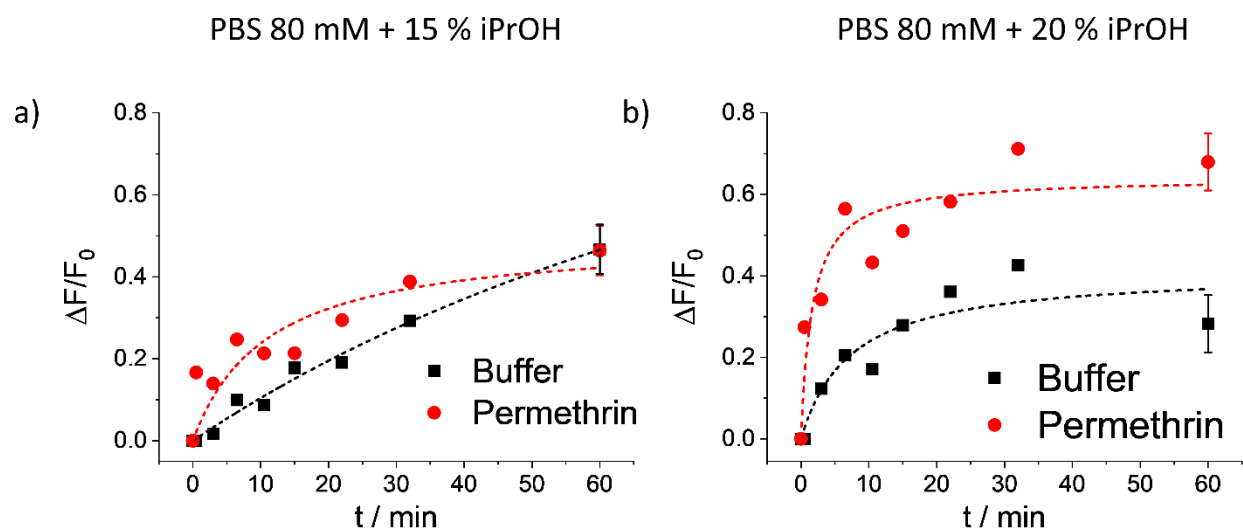


Fig. S3 Fluorescence enhancement registered at 522 nm ($\lambda_{exc} = 490$ nm) for the supernatants in the presence (red) and in the absence (black) of permethrin (6.6 mg kg⁻¹) as a function of time for the suspensions of selected materials S1.1-AB capped with 4 μ L of monoclonal antibody in the presence of BSA in a) PBS (80 mM) containing 15% of iPrOH and b) PBS (80 mM) containing 20% of iPrOH. The lines are included only as a guide to the eye for better illustration.

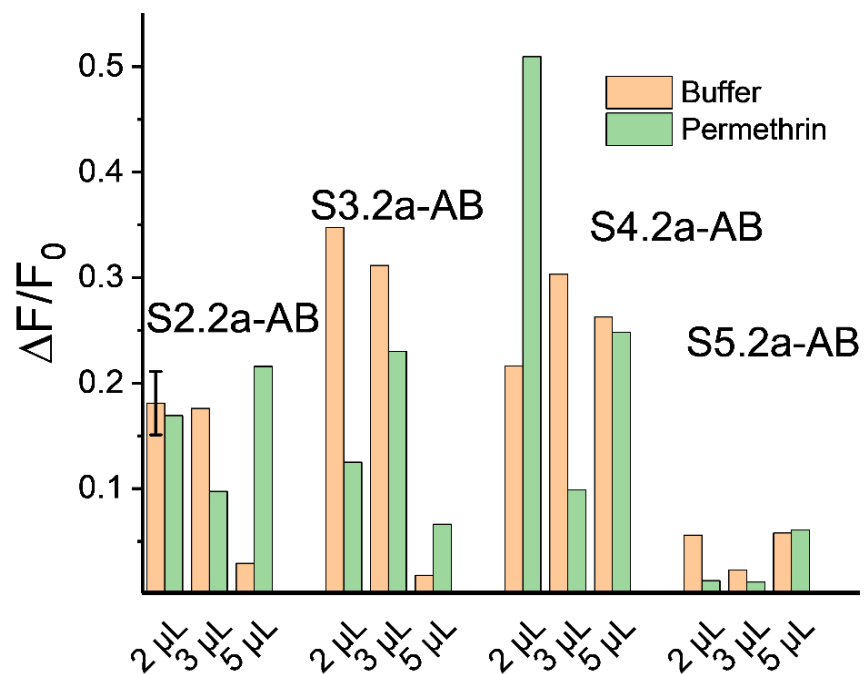


Fig. S4 Fluorescence enhancement as a function of the time of SRG dye released ($\lambda_{\text{exc}} = 532 \text{ nm}$; $\lambda_{\text{em}} = 550 \text{ nm}$) from the corresponding materials in the absence (orange) and in the presence (green) of $500 \mu\text{g kg}^{-1}$ of 3-PBA in phosphate buffer (PBS 80 mM, pH=7.5) containing 10% iPrOH as a function of the amount of antibody used during the capping process.

Analysis of titration data according to binding models. As discussed in the text, the response behaviour of gAID systems is more complex than that for two-partner antibody–antigen or antibody–hapten binding in for instance, classical ELISA. The EC50 value which can be derived from a four-parametric logistic fit of titration data thus cannot be considered as binding constant but is determined (at least) by (i) the affinity between grafted hapten and antibody, especially by the dissociation constant of that complex, (ii) the affinity between antibody and analyte, especially by the association constant of that complex, (iii) transport/diffusion kinetics of analyte and (iv) antibody–analyte complex in suspension or in the flow of an LFA, (v) adsorption of the indicator dye to the inner walls of the porous host scaffold and (vi) diffusion kinetics of the dye in the channels. A unified physico-chemical model has not yet been derived. Accordingly, when trying to analyse titration data according to conventional binding models such as Scatchard or Hill,^{7,8} some do not yield meaningful data whereas others allow getting some (apparent) better insight. While Scatchard analysis of our data belonged to the first category, yielding poor fits, Hill analysis of, e.g. **S1.1a-AB**, **S1.2a-AB** and **S2.2a-AB** was acceptable and allowed to obtain the results summarized in Table S2.

Table S2. Overview of interaction data obtained by a four-parametric logistic fit as well as a Hill analysis of titration data of **S1.1a-AB**, **S1.2a-AB** and **S2.2a-AB** with permethrin.

	logEC _{response}	r ²	logK	n	r ²
			Hill	Hill	Hill
S1.1a-AB	6.85	0.976	5.48	0.48	0.874
S1.2a-AB	8.29	0.932	6.82	0.49	0.952
S2.2a-AB	7.55	0.925	6.56	0.45	0.900

These results indicate that, although hapten, antibody and analyte are identical for all systems, pronounced differences result. Moreover, as a Hill analysis according to equation (1) and its linearized version (2)

$$v = n \frac{(KL_{free})^{n_{Hill}}}{1 + (KL_{free})^{n_{Hill}}} \quad (1)$$

$$\log\left(\frac{v}{n-v}\right) = n_{Hill} \log L_{free} + n_{Hill} \log K \quad (2)$$

reveals,⁸ the Hill coefficient n shows values distinctly smaller than 1, hinting at a non-cooperativity of the single processes involved in the ensemble. Future work, for instance, along lines published recently by Xu et al. are necessary to shed more light on the single processes at play.⁹

S4. Relative measurement uncertainties and limits of detection (LOD)

Limits of detection (LOD) were derived according to the so-called “blank method” as $LOD = LOB + 1,645 \cdot SD^{lcs}$,^{10, 11} where LOB is the limit of blanks, according to $LOB = \bar{x}^0 + 1,645 SD^{LOB}$ (SD^{LOB} = standard deviation of blank replicates, \bar{x}^0 = mean of blank replicates), and SD^{lcs} (lcs = low-concentration samples) is the standard deviation obtained from replicate measurements of samples with the (commonly three) lowest known concentrations, assuming a Gaussian distribution and taking a confidence interval of 95%.

In addition, the overall uncertainty budget of the assays in suspension and on the strips was derived as detailed below. Such an uncertainty budget is always helpful to get an overview of the contributions of the single steps of the protocol to the overall measurement uncertainty. Because of the multiplicative and quotient forms of the respective equations and because correlations between the quantities are assumed to be negligible, a summation of the squares of the relative uncertainties was performed.^{12,13}

4.1.- Conventional assay:

4.1.1 Preparation of capped materials and stock solutions:

- a) Weighing of ca. 1 mg of **S1.1**, **S1.2**, **S2.2a**, **S2.2b**, **S3.2a**, **S4.2a** or **S5.2a** (balance Mettler Toledo 1 ± 0.01 mg); $u_{rel}^w = 1\%$
- b) Dissolving in 450 μ L PBS (Eppendorf Reference pipette ± 0.0006 mL); $u_{rel}^d = 0.6\%$
- c) Weighing ca. 10 mg BSA (balance Mettler Toledo 1 ± 0.01 mg); $u_{rel}^{w2} = 0.1\%$
- d) Dissolving in 200 μ L PBS (Eppendorf Reference pipette ± 0.0006 mL) and taking 50 μ L of solution; $u_{rel}^{d2} = 1.2\%$
- e) Washing and dividing the suspension to obtain fractions of 0.33 mg of **S1.1-AB**, **S1.2-AB** or stock solutions of 1 mg mL⁻¹ (PBS 80 mM) of **S2.2a-AB**, **S2.2b-AB**, **S3.2a-AB**, **S4.2a-AB** or **S5.2a-AB** (Eppendorf Reference pipette ± 0.0006 mL); $u_{rel}^{d3} = 0.6\%$.
- f) Weighing of ca. 1 mg of 3-PBA, permethrin, phenothrin or etofenprox (balance Mettler Toledo: ± 0.01 mg); $u_{rel}^{ws} = 1\%$

g) Dissolving in 0.1 mL iPrOH (Eppendorf Reference pipette ± 0.0006 mL) for obtaining 3-PBA, permethrin, phenothrin or etofenprox of 10 g L^{-1} in iPrOH; $u_{rel}^{ds} = 0.6 \%$

h) Diluting of stock solutions in iPrOH for obtaining standard permethrin, phenothrin or etofenprox solutions of 100 mg L^{-1} and 1 mg L^{-1} in iPrOH (Eppendorf Reference pipette ± 0.001 mL); $u_{rel}^{ds2} = 1 \%$

i) Preparing permethrin, phenothrin or etofenprox standards in iPrOH ($100 \mu\text{L}$) from 1 mg L^{-1} solution of standards permethrin, phenothrin or etofenprox 1 mg L^{-1} , by diluting it in iPrOH: Successive dilution of the mother solution: $100 \mu\text{L}$ in $100 \mu\text{L}$ iPrOH; $n \times u_{rel}^{ds3} = n \times (1) \%$; $n = 1; 2\times, n = 2; 4\times, n = 3; 8\times, n = 4; 16, n = 5; 32\times, n = 6; 64\times, n = 7; 128\times, n = 8; 256\times, n = 9; 512\times, n = 10; 1024\times, n = 11; 2048\times, n = 12; 4096\times, n = 13; 8192\times$.

4.1.2 Assay execution and preparation of measurement solutions:

a) Mixing 0.33 mL capped material (1 mg mL^{-1} in PBS 80 mM) with 2.2 mL PBS (Eppendorf Reference pipette ± 0.00625 mL); $u_{rel}^{d4} = 1.2 \%$

b) Fractionation of the suspension (0.14 mL) (Eppendorf Reference pipette ± 0.0006 mL); $u_{rel}^{d5} = 0.6 \%$

c) Addition $16 \mu\text{L}$ Ci in iPrOH (Eppendorf Reference pipette ± 0.0003 mL); $u_{rel}^{d6} = 2 \%$

d) Transfer of the fractions into a 10 mm optical path length quartz cell (optically active volume of $3 \times 15 \times 10 \text{ mm}$). Since no dilution step is involved, only contribution from cell length ($\pm 0.01 \text{ mm}$); $u_{rel}^L = 0.1 \%$

4.1.3 Fluorescence measurements:

a) Relative uncertainty of the emission spectrum across the respective wavelength range: $u_{rel}^f \leq 5 \%$

b) For the fluorescence intensities at λ_i , the maximum possible error amounts to; $u_{rel}^{f2} \leq 0.05 \%$

4.1.4 Experimental standard deviation for replicate measurements: $u_{rel}^s \leq 7.8 \%$

4.1.5 Relative uncertainty: $u_{rel}^u \leq 9.8 \%$

$$\text{Relative uncertainty : } u_{rel}^2 = u_{rel}^w{}^2 + u_{rel}^d{}^2 + u_{rel}^{w2}{}^2 + u_{rel}^{d2}{}^2 + u_{rel}^{d3}{}^2 + u_{rel}^{ws}{}^2 + u_{rel}^{ds}{}^2 + u_{rel}^{ds2}{}^2 + n * u_{rel}^{ds3}{}^2 + u_{rel}^{d4}{}^2 + u_{rel}^{d5}{}^2 + u_{rel}^{d6}{}^2 + u_{rel}^L{}^2 + u_{rel}^f{}^2 + u_{rel}^{f2}{}^2 + u_{rel}^s{}^2 + u_{rel}^u{}^2$$

Table S3. Calculation of relative errors in a conventional assay in suspension

Solutions	Relative error of the measurement	%
Standard	$u_{rel}^2 = u_{rel}^w{}^2 + u_{rel}^d{}^2 + u_{rel}^{w2}{}^2 + u_{rel}^{d2}{}^2 + u_{rel}^{d3}{}^2 + u_{rel}^{ws}{}^2 + u_{rel}^{ds}{}^2 + u_{rel}^{ds2}{}^2 + 0 * u_{rel}^{ds3}{}^2 + u_{rel}^{d4}{}^2 + u_{rel}^{d5}{}^2 + u_{rel}^{d6}{}^2 + u_{rel}^L{}^2 + u_{rel}^f{}^2 + u_{rel}^{f2}{}^2 + u_{rel}^s{}^2 + u_{rel}^u{}^2$	9.0
8x	$u_{rel}^2 = u_{rel}^w{}^2 + u_{rel}^d{}^2 + u_{rel}^{w2}{}^2 + u_{rel}^{d2}{}^2 + u_{rel}^{d3}{}^2 + u_{rel}^{ws}{}^2 + u_{rel}^{ds}{}^2 + u_{rel}^{ds2}{}^2 + 3 * u_{rel}^{ds3}{}^2 + u_{rel}^{d4}{}^2 + u_{rel}^{d5}{}^2 + u_{rel}^{d6}{}^2 + u_{rel}^L{}^2 + u_{rel}^f{}^2 + u_{rel}^{f2}{}^2 + u_{rel}^s{}^2 + u_{rel}^u{}^2$	9.2
64x	$u_{rel}^2 = u_{rel}^w{}^2 + u_{rel}^d{}^2 + u_{rel}^{w2}{}^2 + u_{rel}^{d2}{}^2 + u_{rel}^{d3}{}^2 + u_{rel}^{ws}{}^2 + u_{rel}^{ds}{}^2 + u_{rel}^{ds2}{}^2 + 6 * u_{rel}^{ds3}{}^2 + u_{rel}^{d4}{}^2 + u_{rel}^{d5}{}^2 + u_{rel}^{d6}{}^2 + u_{rel}^L{}^2 + u_{rel}^f{}^2 + u_{rel}^{f2}{}^2 + u_{rel}^s{}^2 + u_{rel}^u{}^2$	9.4
512x	$u_{rel}^2 = u_{rel}^w{}^2 + u_{rel}^d{}^2 + u_{rel}^{w2}{}^2 + u_{rel}^{d2}{}^2 + u_{rel}^{d3}{}^2 + u_{rel}^{ws}{}^2 + u_{rel}^{ds}{}^2 + u_{rel}^{ds2}{}^2 + 9 * u_{rel}^{ds3}{}^2 + u_{rel}^{d4}{}^2 + u_{rel}^{d5}{}^2 + u_{rel}^{d6}{}^2 + u_{rel}^L{}^2 + u_{rel}^f{}^2 + u_{rel}^{f2}{}^2 + u_{rel}^s{}^2 + u_{rel}^u{}^2$	9.6
4096x	$u_{rel}^2 = u_{rel}^w{}^2 + u_{rel}^d{}^2 + u_{rel}^{w2}{}^2 + u_{rel}^{d2}{}^2 + u_{rel}^{d3}{}^2 + u_{rel}^{ws}{}^2 + u_{rel}^{ds}{}^2 + u_{rel}^{ds2}{}^2 + 12 * u_{rel}^{ds3}{}^2 + u_{rel}^{d4}{}^2 + u_{rel}^{d5}{}^2 + u_{rel}^{d6}{}^2 + u_{rel}^L{}^2 + u_{rel}^f{}^2 + u_{rel}^{f2}{}^2 + u_{rel}^s{}^2 + u_{rel}^u{}^2$	9.8

4.2 Lateral flow assay

4.2.1 Preparation of suspensions and stock solutions:

- a) Weighing of ca. 1 mg of **S1.1**, **S1.2**, **S2.2a**, **S2.2b**, **S3.2a**, **S4.2a** or **S5.2a** (balance Mettler Toledo 1 ± 0.01 mg); $u_{rel}^w = 1\%$
- b) Dissolving in 450 μ L PBS (Eppendorf Reference pipette ± 0.0006 mL); $u_{rel}^d = 0.6\%$
- c) Weighing ca. 10 mg BSA (balance Mettler Toledo 1 ± 0.01 mg); $u_{rel}^{w2} = 0.1\%$
- d) Dissolving in 200 μ L PBS (Eppendorf Reference pipette ± 0.0006 mL) and taking 50 μ L of solution; $u_{rel}^{d2} = 1.2\%$
- e) Washing and dividing the suspension to obtain 1 mg mL⁻¹ (PBS 80 mM) of stock solutions of **S1.2-AB**, **S2.2a-AB**, **S2.2b-AB**, **S3.2a-AB**, **S4.2a-AB** or **S5.2a-AB** (Eppendorf Reference pipette ± 0.0006 mL); $u_{rel}^{d3} = 0.6\%$.
- f) Weighing of ca. 1 mg of 3-PBA, permethrin, phenothrin or etofenprox (balance Mettler Toledo: ± 0.01 mg); $u_{rel}^{ws} = 1\%$
- g) Dissolving in 0.1 mL iPrOH (Eppendorf Reference pipette ± 0.0006 mL) for obtaining 3-PBA, permethrin, phenothrin or etofenprox of 10 g L⁻¹ in iPrOH; $u_{rel}^{ds} = 0.6\%$
- h) Diluting of stock solutions in iPrOH for obtaining standard permethrin, phenothrin or etofenprox solutions of 100 mg L⁻¹ in PBS : iPrOH (99:1, Eppendorf Reference pipette ± 0.001 mL); $u_{rel}^{ds2} = 3\%$
- i) Preparing permethrin, phenothrin or etofenprox standards in PBS containing iPrOH (500 μ L) from 100 mg L⁻¹ solution of standards permethrin, phenothrin or etofenprox 1 mg L⁻¹, by diluting it in PBS: Successive dilution of the mother solution: 100 μ L in 100 μ L in PBS : iPrOH (99:1); $n \times u_{rel}^{ds3} = n \times (1)\%$; n = 1; 2 \times , n = 2; 4 \times , n = 3; 8 \times , n = 4; 16, n = 5; 32 \times , n = 6; 64 \times , n = 7; 128 \times , n = 8; 256 \times , n = 9; 512 \times , n = 10; 1024 \times , n = 11; 2048 \times , n = 12; 4096 \times , n = 13; 8192 \times .

4.2.2 Strip preparation:

- a) Deposition of 2.5 μ L of suspension onto the strip (Eppendorf Reference pipette ± 0.00003 mL); $u_{rel}^{d2} = 1.4\%$

4.2.3 Integration of the signal using ImageJ:

a) Relative uncertainty of the fluorescence intensities. $u_{rel}^c \leq 5\%$

4.2.4 Experimental standard deviation for replicate measurements: $u_{rel}^{sc} \leq 5\%$

4.2.5 Relative uncertainty: $u_{rel}^u \leq 7.1\%$

Relative uncertainty : $u_{rel}^2 = u_{rel}^w{}^2 + u_{rel}^d{}^2 + u_{rel}^{w2}{}^2 + u_{rel}^{d2}{}^2 + u_{rel}^{d3}{}^2 + u_{rel}^{ws}{}^2 + u_{rel}^{ds}{}^2 + u_{rel}^{ds2}{}^2 +$
 $n * u_{rel}^{ds3}{}^2 + u_{rel}^{d2}{}^2 + u_{rel}^c{}^2 + u_{rel}^{sc}{}^2$

Table S4. Calculation of relative errors in a lateral flow assay using a camera

Solutions	Relative error of the measurement	%
Standard	$u_{rel}^2 = u_{rel}^w{}^2 + u_{rel}^d{}^2 + u_{rel}^{w2}{}^2 + u_{rel}^{d2}{}^2 + u_{rel}^{d3}{}^2 + u_{rel}^{ws}{}^2 + u_{rel}^{ds}{}^2 + u_{rel}^{ds2}{}^2$ $+ 0 * u_{rel}^{ds3}{}^2 + u_{rel}^{d2}{}^2 + u_{rel}^c{}^2 + u_{rel}^{sc}{}^2$	6.2
8x	$u_{rel}^2 = u_{rel}^w{}^2 + u_{rel}^d{}^2 + u_{rel}^{w2}{}^2 + u_{rel}^{d2}{}^2 + u_{rel}^{d3}{}^2 + u_{rel}^{ws}{}^2 + u_{rel}^{ds}{}^2 + u_{rel}^{ds2}{}^2$ $+ 3 * u_{rel}^{ds3}{}^2 + u_{rel}^{d2}{}^2 + u_{rel}^c{}^2 + u_{rel}^{sc}{}^2$	6.5
64x	$u_{rel}^2 = u_{rel}^w{}^2 + u_{rel}^d{}^2 + u_{rel}^{w2}{}^2 + u_{rel}^{d2}{}^2 + u_{rel}^{d3}{}^2 + u_{rel}^{ws}{}^2 + u_{rel}^{ds}{}^2 + u_{rel}^{ds2}{}^2$ $+ 6 * u_{rel}^{ds3}{}^2 + u_{rel}^{d2}{}^2 + u_{rel}^c{}^2 + u_{rel}^{sc}{}^2$	6.7
512x	$u_{rel}^2 = u_{rel}^w{}^2 + u_{rel}^d{}^2 + u_{rel}^{w2}{}^2 + u_{rel}^{d2}{}^2 + u_{rel}^{d3}{}^2 + u_{rel}^{ws}{}^2 + u_{rel}^{ds}{}^2 + u_{rel}^{ds2}{}^2$ $+ 9 * u_{rel}^{ds3}{}^2 + u_{rel}^{d2}{}^2 + u_{rel}^c{}^2 + u_{rel}^{sc}{}^2$	6.9
4096x	$u_{rel}^2 = u_{rel}^w{}^2 + u_{rel}^d{}^2 + u_{rel}^{w2}{}^2 + u_{rel}^{d2}{}^2 + u_{rel}^{d3}{}^2 + u_{rel}^{ws}{}^2 + u_{rel}^{ds}{}^2 + u_{rel}^{ds2}{}^2$ $+ 12 * u_{rel}^{ds3}{}^2 + u_{rel}^{d2}{}^2 + u_{rel}^c{}^2 + u_{rel}^{sc}{}^2$	7.1

S5. NMR and MS spectra

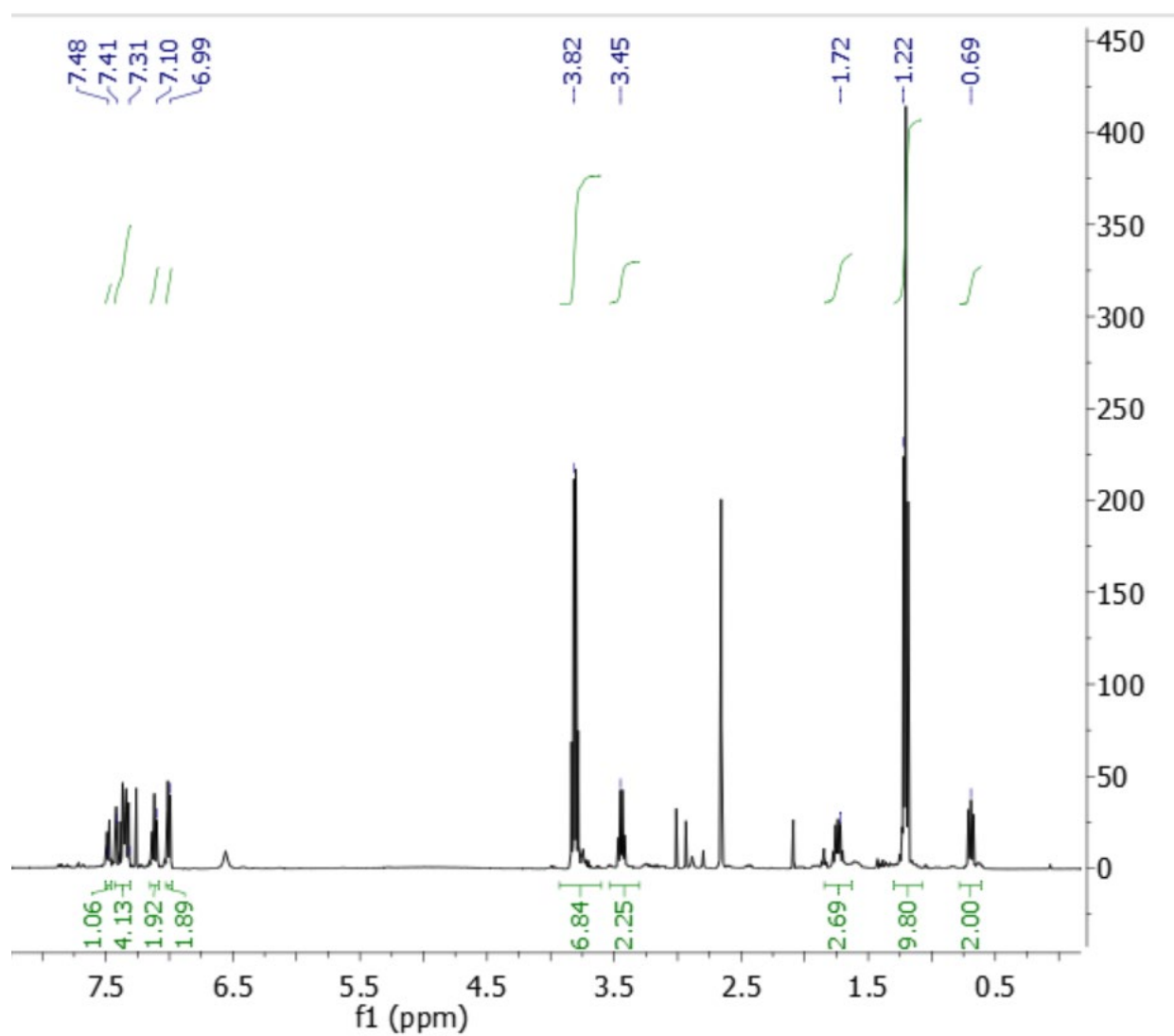


Fig. S5. ^1H NMR spectrum of 3-phenoxybenzoic acid silane derivative I (CDCl_3 , 400 MHz); traces of residual CHCl_3 and THF still contained as thorough clean-up was not attempted to avoid hydrolysis.

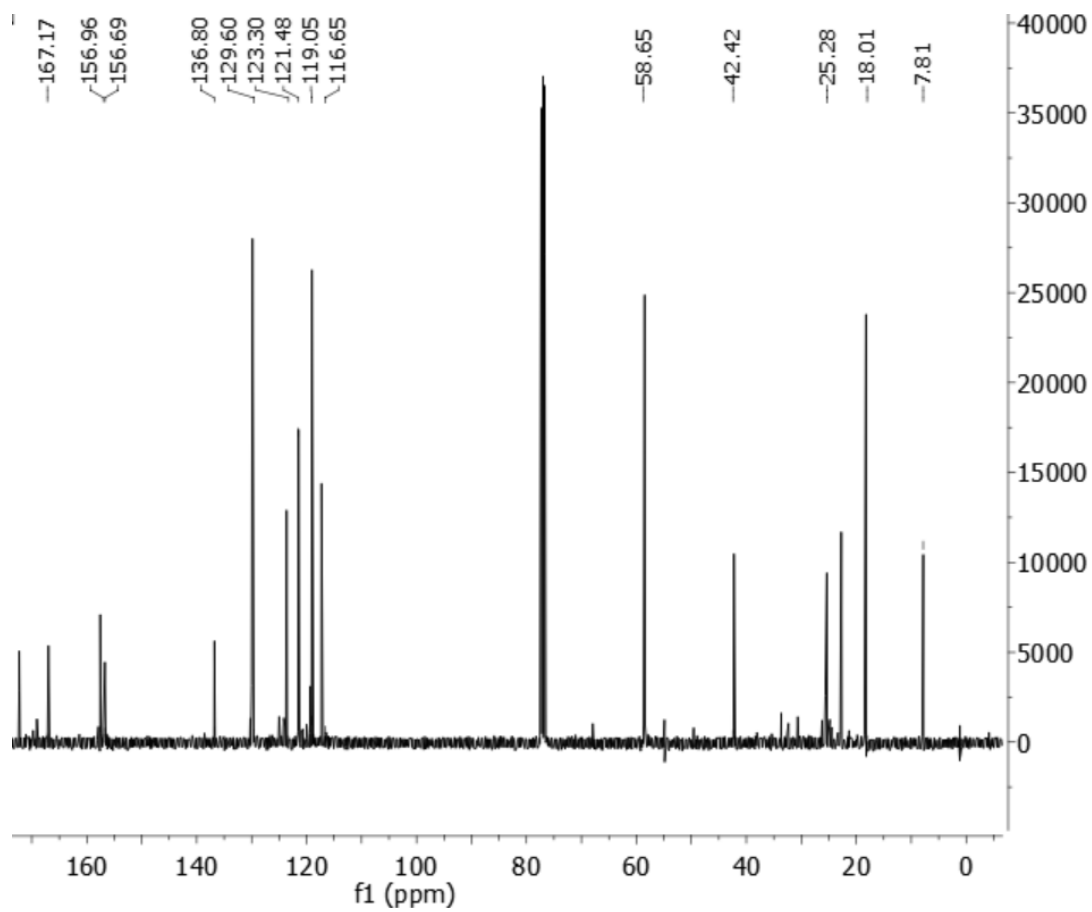


Fig. S6. ¹³C NMR spectrum of 3-phenoxybenzoic acid silane derivative I (CDCl₃, 400 MHz); traces of residual CHCl₃ and THF still contained as thorough clean-up was not attempted to avoid hydrolysis.

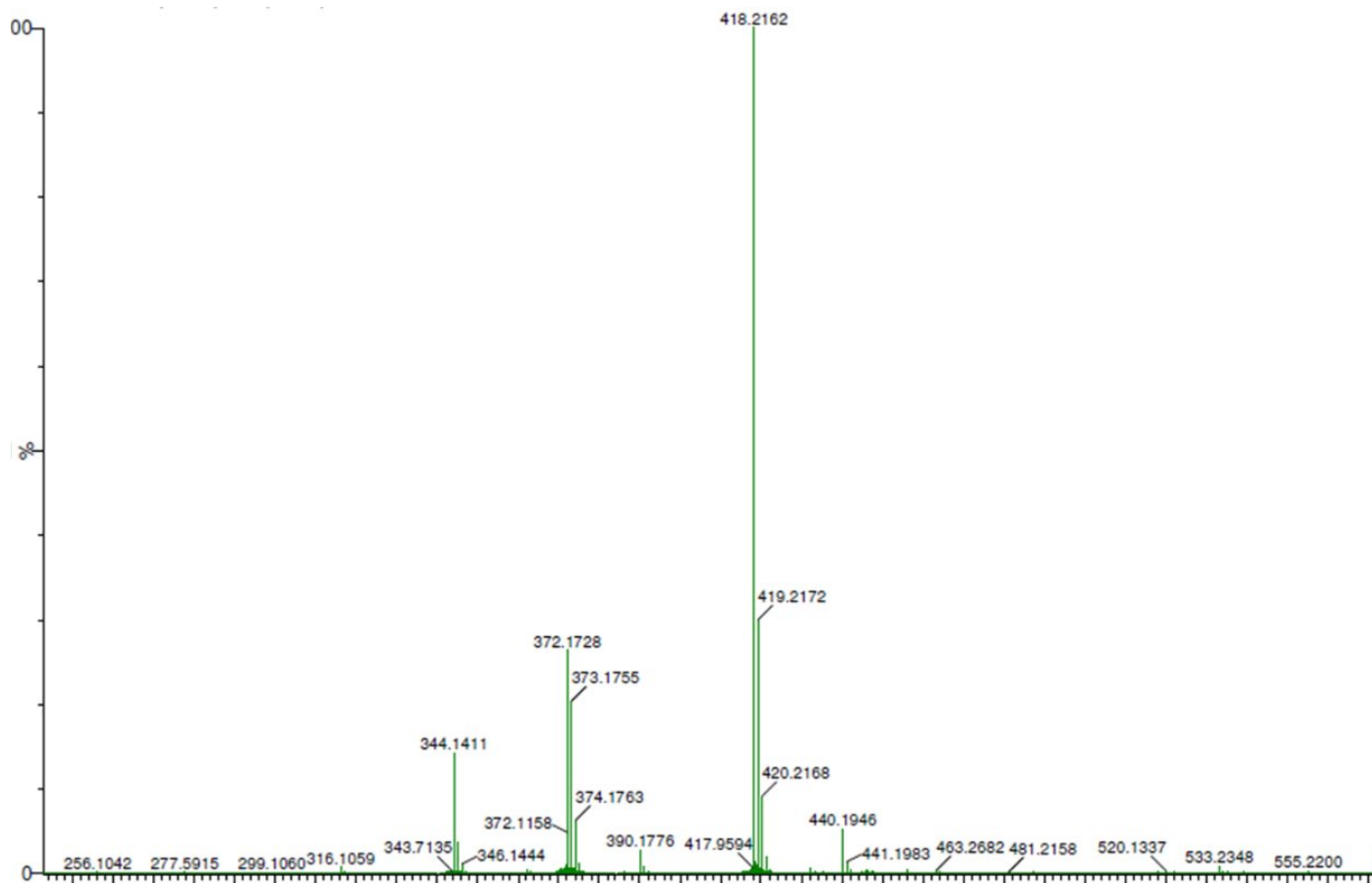


Fig. S7. Mass spectrum of 3-phenoxybenzoic acid silane derivative I (exact mass $C_{20}H_{32}NO_3Si$ $[M+H]^+$ 418.2050).

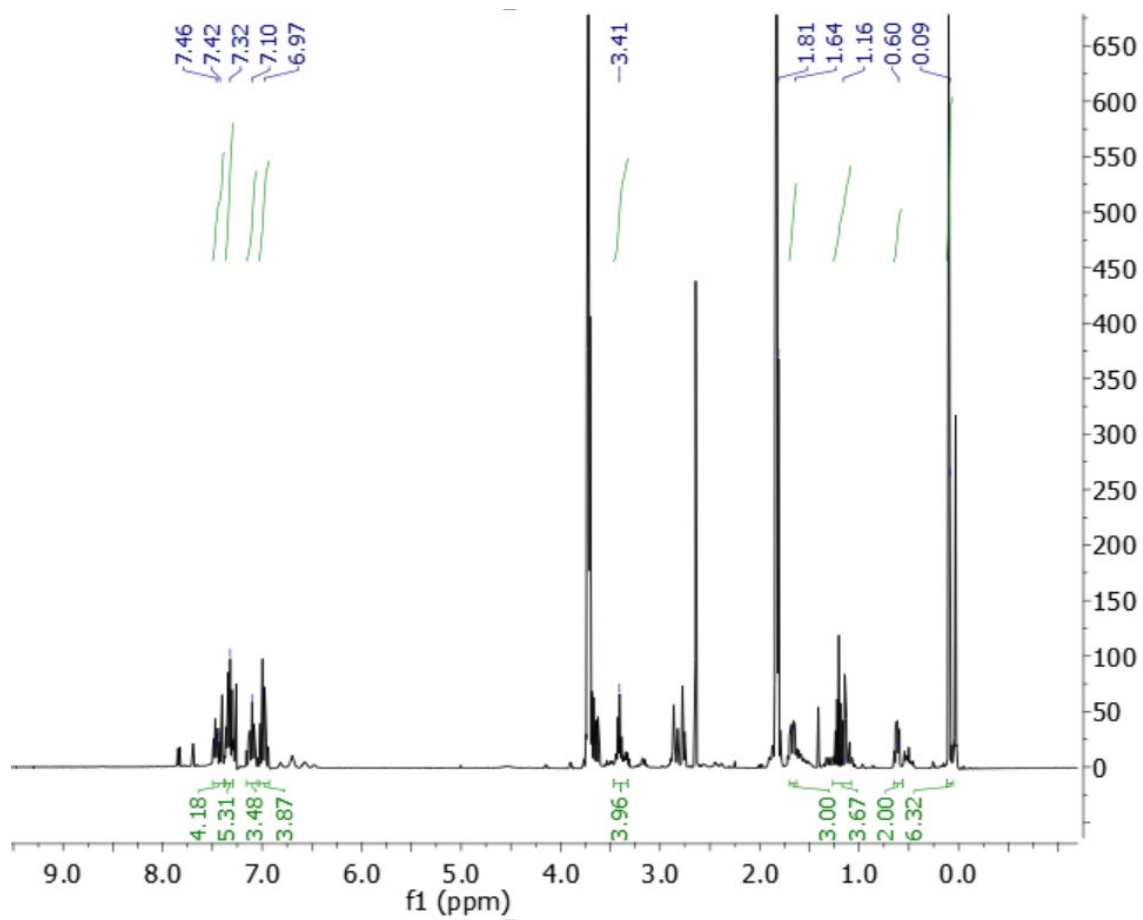


Fig. S8. ^1H NMR spectrum of 3-phenoxybenzoic acid silane derivative **II** (CDCl_3 , 400 MHz); traces of residual CHCl_3 and THF still contained as thorough clean-up was not attempted to avoid hydrolysis.

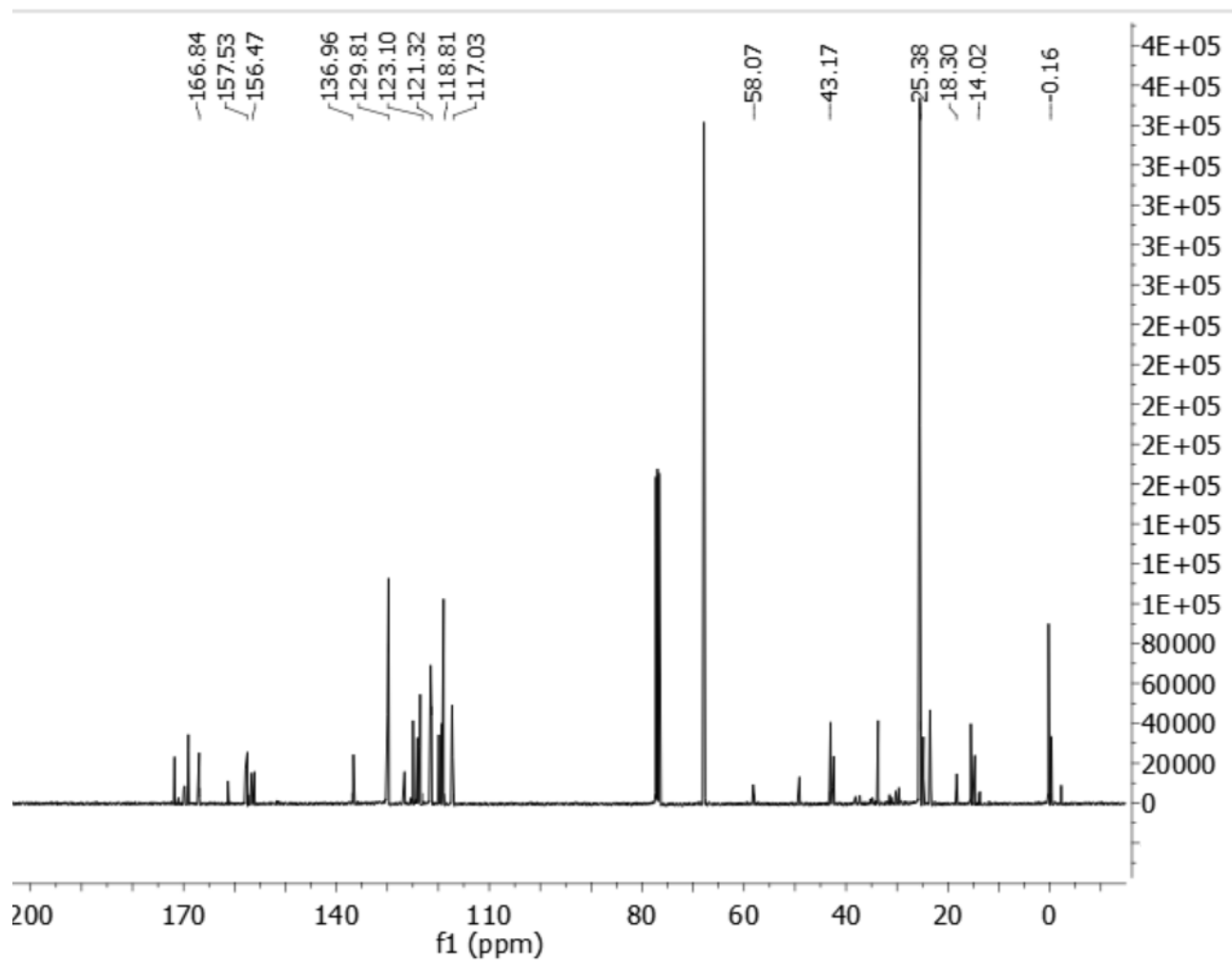


Fig. S9. ^{13}C NMR spectrum of 3-phenoxybenzoic acid silane derivative II (CDCl_3 , 400 MHz); traces of residual CHCl_3 and THF still contained as thorough clean-up was not attempted to avoid hydrolysis.

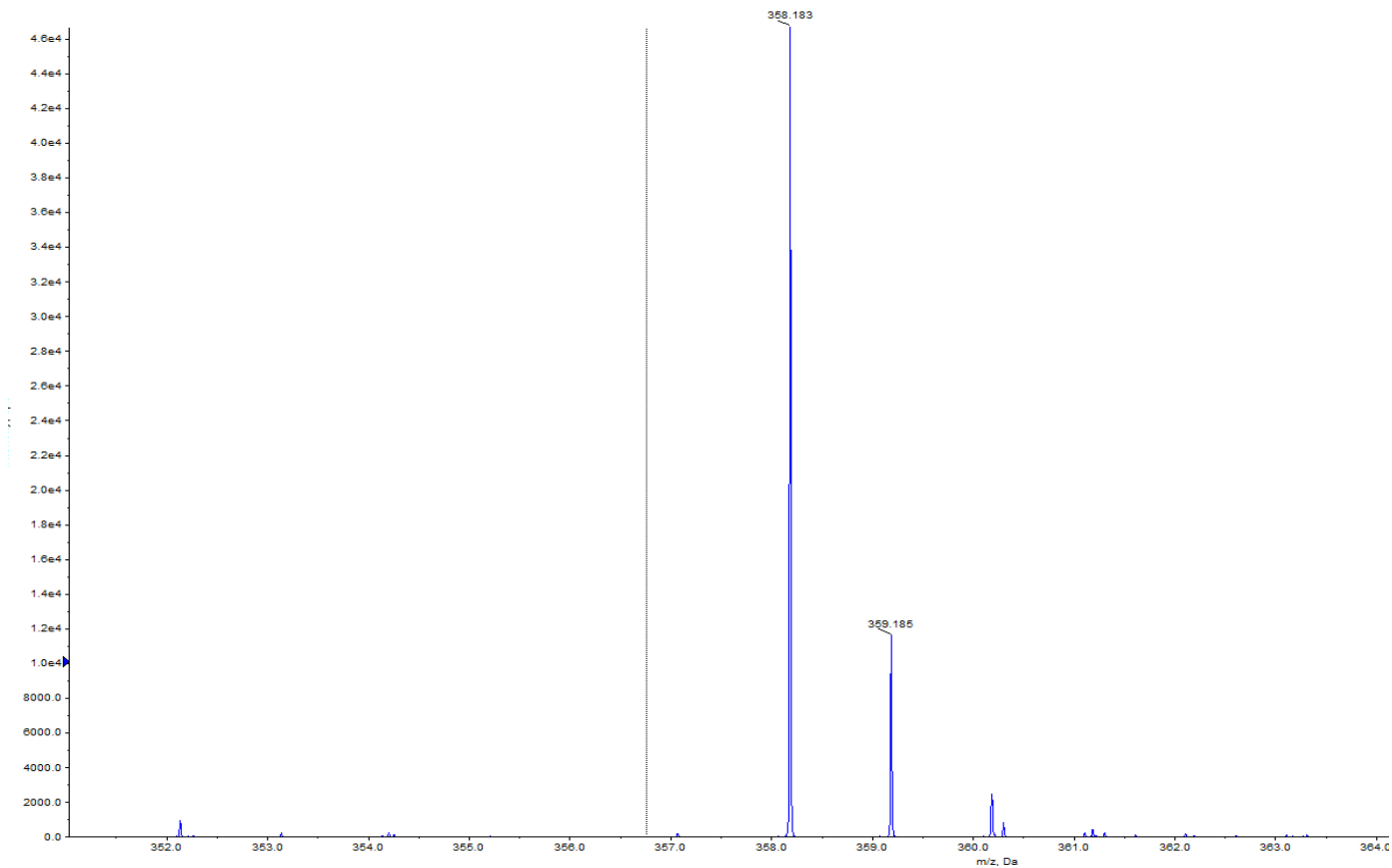


Fig. S10. Mass spectrum of 3-phenoxybenzoic acid silane derivative II (exact mass $C_{20}H_{28}NO_3Si$ $[M+H]^+$ 358.1838).

S6. References

1. E. Costa, E. Climent, S. Ast, M. G. Weller, J. Canning and K. Rurack, *Analyst*, 2020, DOI: 10.1039/D0AN00319K.
2. T. Watanabe, G. Shan, D. W. Stoutamire, S. J. Gee and B. D. Hammock, *Anal. Chim. Acta*, 2001, **444**, 119-129.
3. Q. Cai, Z.-S. Luo, W.-Q. Pang, Y.-W. Fan, X.-H. Chen and F.-Z. Cui, *Chem. Mater.*, 2001, **13**, 258-263.
4. S.-Y. Chen, C.-Y. Tang, W.-T. Chuang, J.-J. Lee, Y.-L. Tsai, J. C. C. Chan, C.-Y. Lin, Y.-C. Liu and S. Cheng, *Chem. Mater.*, 2008, **20**, 3906-3916.
5. S.-Y. Chen, Y.-T. Chen, J.-J. Lee and S. Cheng, *J. Mater. Chem.*, 2011, **21**, 5693-5703.
6. G. F. Andrade, D. C. F. Soares, R. G. dos Santos and E. M. B. Sousa, *Microporous Mesoporous Mater.*, 2013, **168**, 102-110.
7. G. Scatchard, *Ann. N.Y. Acad. Sci.*, 1949, **51**, 660-672.
8. A. V. Hill, *J. Physiol.*, 1910, **40**, iv-vii.
9. G. K. Xu, J. L. Hu, R. Lipowsky and T. R. Weikl, *J. Chem. Phys.*, 2015, **143**.
10. *DIN 32645:2008-11, Chemical analysis - Decision limit, detection limit and determination limit under repeatability conditions - Terms, methods, evaluation*, 2008.
11. D. A. Armbruster and T. Pry, *Clin. Biochem. Rev.*, 2008, **29**, S49-S52.
12. *Evaluation of Measurement Data—Guide to the Expression of Uncertainty in Measurement*; Joint Committee for Guides in Metrology JCGM, Paris, 1 Edn, 2008, corrected version 2010.
13. B. Walter, G. C. Maurice and M. H. Peter, *Metrologia*, 2006, **43**, S161.